Astronomical Techniques and Instruments, Vol. 1, March 2024, 140–149

Article Open Access

HF-VHF dual-channel multifunctional radio astronomy terminal system

Kaijing Liu[1], Liang Dong[2,4*], Huanhuan Xie[3,4], Baoxin Li[3,4], Jingzhi Zhou[1]

[1]*School of Information Engineering*, *Southwest University of Science and Technology*, *Mianyang* 621010, *China*

[2]*Yunnan Observatories*, *Chinese Academy of Sciences*, *Kunming* 650216, *China*

[3]*Xi'an Research Institute of Navigation Technology*, *Xi'an* 710068, *China*

[4]*Yunnan Province China-Malaysia HF-VHF Advanced Radio Astronomy Technology International Joint Laboratory*, *Kunming* 650216, *China*

*Correspondence: dongliang@ynao.ac.cn

Received: December 5, 2023; Accepted: January 12, 2024; Published Online: March 6, 2024; https://doi.org/10.61977/ati2024011

Citation: Liu, K. J., Dong, L., Xie, H. H., et al. 2024. HF-VHF dual-channel multifunctional radio astronomy terminal system. *Astronomical Techniques and Instruments*, **1**(2): 140−149. https://doi.org/10.61977/ati2024011.

Abstract: The high frequency-very high frequency (HF-VHF) frequency band is of significant importance in astronomical observations, with applications studying various phenomena such as space weather, solar radio emissions, planetary eruptions in the solar system, pulsars, transient sources, and reionization of the early universe. This article introduces the HF-VHF frequency band multifunctional radio astronomical terminal system based on a dual-channel high-speed acquisition board with a frequency observation range of 1−250 MHz and a sampling rate of 500 Msps (Mega samples per second). The maximum quantization bit of the system is 14 bits, with a maximum time resolution of 0.1 s and a maximum spectral resolution of 16 kHz. The system combines spectral analysis of solar radio signals and recording of time-domain data of signals interfering with long baselines, and adopts a server-client separation mode to allow remote operation with separate permissions. It is used in the China-Malaysia joint astronomy project, which can carry out single-site observation of solar radio signals as well as interferometric observation of signals from multiple sites.

Keywords: HF-VHF; Solar radio; High-speed acquisition; Frequency domain analysis; Time-domain recording.

1. INTRODUCTION

According to international telecommunication union (ITU) classifications, the high frequency (HF) and very high frequency (VHF) bands refer to the frequency ranges in the radio spectrum from 3 MHz to 30 MHz and from 30 MHz to 300 MHz[1], respectively. Solar flares release a substantial amount of radio emission, with higher intensity in the HF-VHF frequency range. This radiation provides vital information about solar activities, solar wind, and related phenomena[2,3]. Consequently, astronomers observe solar radio emissions in the HF-VHF frequency range to study solar activities, the release of energy during solar flares[4]. Furthermore, HF-VHF radio observations are also used to investigate various other astronomical phenomena such as the large-scale high-resolution radiation characteristics of the Milky Way galaxy, surveys of galactic ionized hydrogen distribution, and the time-varying frequency characteristics of transient celestial objects[5-9].

The HF-VHF frequency bands encompass a rich variety of celestial phenomena and radiation, but there has been a limited focus on such observations within China. To address this observational gap, this paper introduces a dual-channel multifunctional radio astronomy terminal system for the HF-VHF frequency band. This system facilitates spectral analysis of solar radio emissions and time-domain recording for long-baseline interferometry. The dual-channel configuration allows for the simultaneous observation and processing of both vertically and horizontally polarized signals, thereby enhancing observational efficiency and flexibility. Furthermore, in conjunction with a server-client separation model, this system enables remote solar radio signal observations and data sharing with varying permission levels.

2. RADIO ASTRONOMY TERMINAL SYSTEM COMPONENTS

2.1. Observation System Components

The HF-VHF dual-channel multifunctional radio astronomy terminal system comprises four main components: the data processing unit, control unit, antenna time-frequency unit, and storage unit. The antenna system and receiving structure serve as the signal inputs, and the entire system is depicted in Fig. 1.

Functioning as the interface between the electromagnetic waves propagating through space and the electronic components of a system, antennas play a pivotal role in capturing and converting electromagnetic signals for further processing. In the HF-VHF frequency bands, antenna arrays are employed to achieve high-gain electromagnetic signal tracking, converting electromagnetic waves into current signals for processing by the system. The receiver is responsible for amplifying the current signals transmitted from the antenna, subsequently forwarding them to the backend data processing unit, which is tasked with processing, and analyzing the analog signals obtained from the receiver.

The control unit functions as the central component of the system, coordinating the operations of various functional units. The antenna time-frequency unit provides the entire system with standard time and reference frequency using high-precision clock sources. The storage unit uses a disk array to store a large amount of observation data. It combines hard disk drives (HDDs) and solid state drives (SSDs) together through tiered storage. HDDs are used to provide high-capacity, relatively low-cost storage, while SSDs are used to provide storage with faster performance and low latency.

This article primarily focuses on the data processing unit. Given the provision of standard time and reference frequency by the time-frequency unit, the data processing unit is responsible for converting radio signals from 1 to 250 MHz output by the receiver into electrical signals. These signals are subsequently digitized into default 14-bit digital signals by analog-to-digital converter (ADC). Following this step, the digital signals undergo various processing tasks such as signal windowing, fast Fourier transform (FFT), power spectrum computation, and power spectrum averaging. Finally, the timestamped data are transmitted to the client and stored via gigabit Ethernet in user datagram protocol (UDP) format. This process achieves the integration of ADC, data processing, storage, and data upload.

2.2. Hardware Structure of the System's Data Processing Unit

The data acquisition board of the system primarily consists of the Power Module, RS232 Serial Port Module, Clock Module, field-programmable gate array (FPGA) Module, ADC Module, and various interfaces. The host computer communicates with the data acquisition board by sending control parameters via peripheral component interconnect express (PCI-Express). The data acquisition board, equipped with a high-capacity FPGA module, preprocesses the signals received from the ADC module using techniques including digital down-conversion (DDC) and FFT. The FPGA module and the ADC module are interconnected via low-voltage differential signaling (LVDS), allowing for raw data buffering of up to 1 s. Spectral and raw

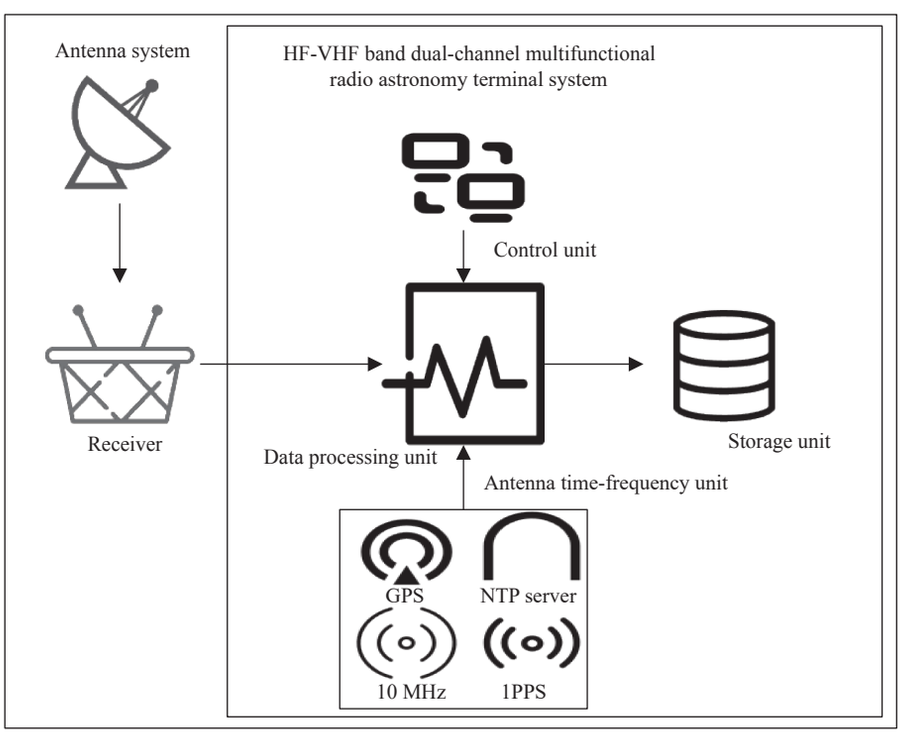

Fig. 1. Schematic diagram of observation system components.

data can be transmitted to the host computer software via the PCI-Express bus for storage and post-processing. The hardware composition of the data acquisition board is illustrated in Fig. 2.

2.2.1. *FPGA module*

The FPGA module uses the XC7K410T_2FFG900I chip from Xilinx's high-performance, low-power Kintex-7 series. This chip features 31 775 logic array blocks (LAB)/configurable logic block (CLBs), 406 720 logic elements/units, and a total of 29 306 880 bits of random access memory (RAM). The chip has 500 input/output (I/O), including 350 high-speed reconfigurable I/O (HRIO) and 150 high performance I/O (HPIO), which accommodate the system's data interaction requirements with various components such as serial ports, double data rate (DDR), flash memory, triggers, ADC, clocks, and PCI-Express.

The high-speed interface for the FPGA module is the gigabit transceiver (GTX) interface, supporting a maximum data rate of 12.5 Gbps. One GTX bank is dedicated to the PCI-Express interface, which operates as an x8 interface, meeting the requirements of the HF-VHF dual-channel multifunctional radio astronomy terminal system, where each channel must have a sampling rate of no less than 500 Msps .

The flash drive configuration for the FPGA module uses Micron's N25Q256A13EF840F flash drive, which is a non-volatile serial NOR flash ("Not OR" Flash) memory device. It has a storage capacity of 256 MB and supports a clock frequency of up to 54 MHz under quad I/O instructions. This chip fulfills the requirements for programming and loading programs onto the system's data acquisition board.

2.2.2. *ADC module*

The ADC module design incorporates the AD9684BBPZ-500 chip, a dual-channel, 14-bit, 500 Msps digitizer. This module is equipped with on-chip buffers and sample-and-hold circuits, optimized for wide input bandwidth, high sampling rates, exceptional linearity, compact packaging, and low power consumption. Its signal distribution diagram is illustrated in Fig. 3, meeting the requirements for high-speed sampling, high data throughput, and high-performance deployment of the HF-VHF dual-channel multifunctional radio astronomy terminal system.

2.2.3. *Clock module*

The signal distribution for the clock module is shown

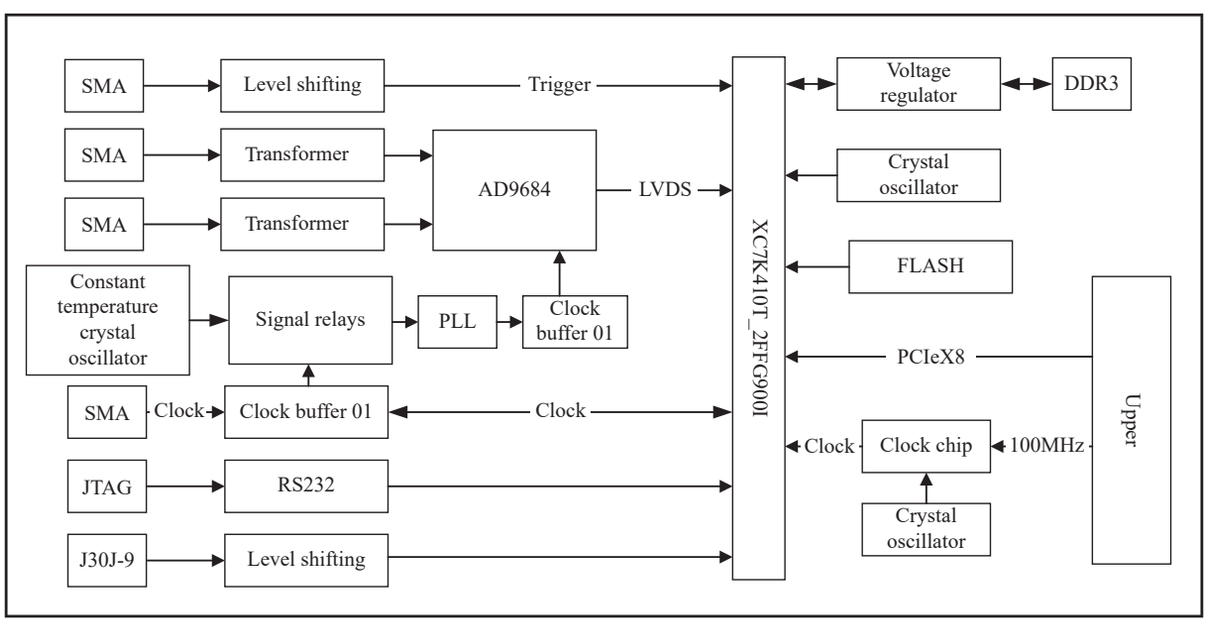

Fig. 2. Diagram showing the architecture of the data acquisition board hardware.

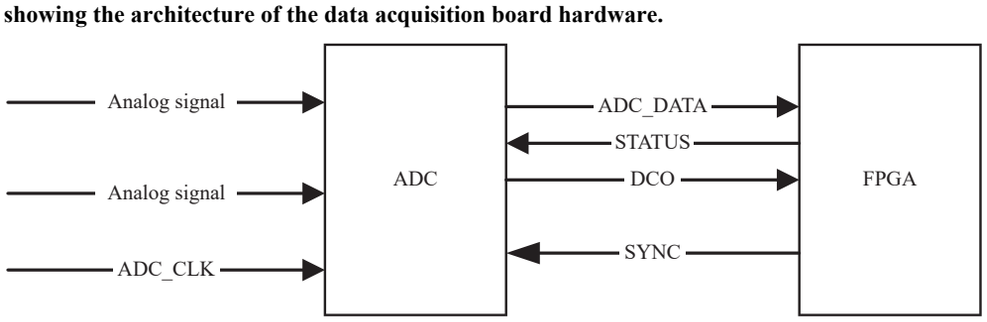

Fig. 3. ADC block signal distribution plot.

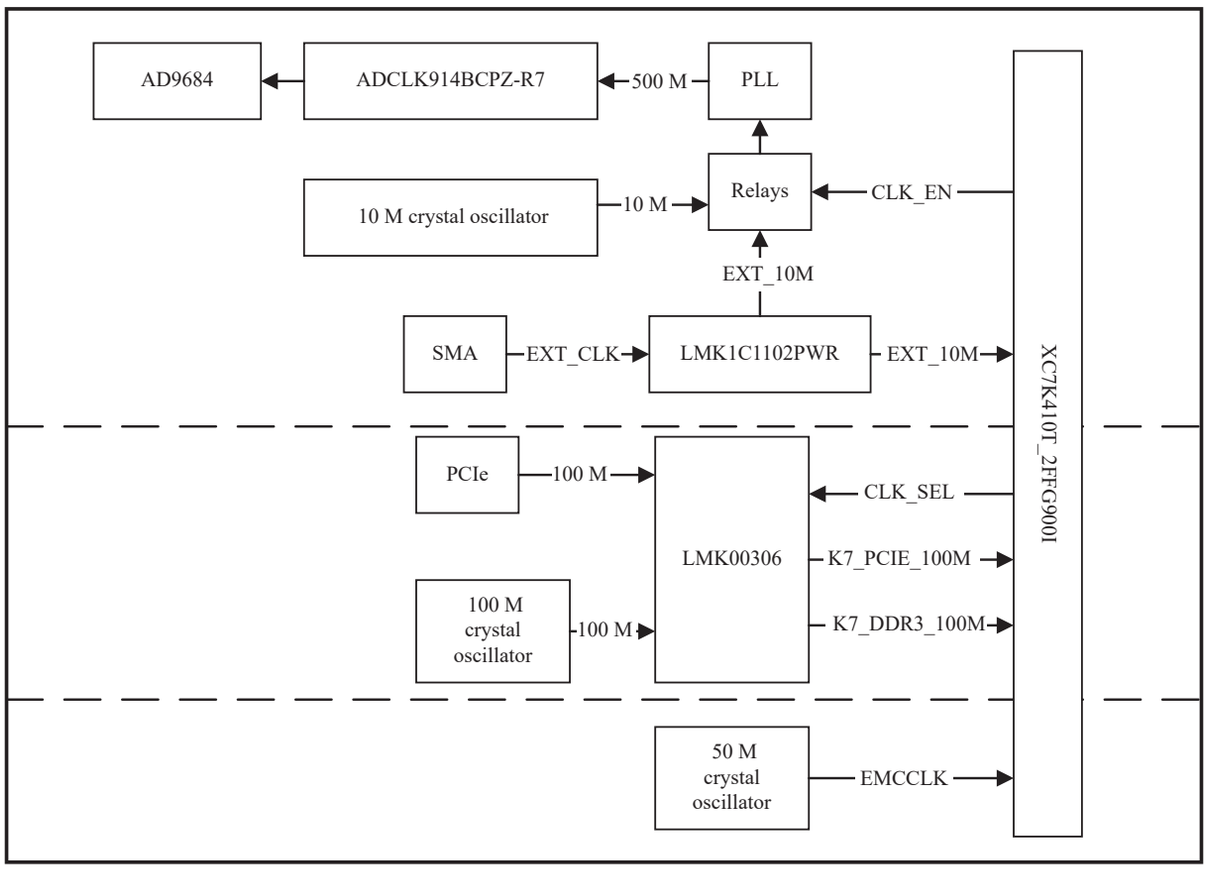

Fig. 4. Clock module signal distribution.

in Fig. 4. One path uses an external clock through an subminiature version A (SMA) interface as the reference clock input, which is then split into two groups. One group provides clock signals to the FPGA, allowing the FPGA to control relays via clock enable signals. The other group is connected to the ADC chip via relays and uses the 10 MHz signal from the crystal oscillator to provide a 500 MHz clock signal to the ADC. In addition, another path employs the LMK00306SQE/NOPB clock buffer, which can select input clocks from two general inputs or one crystal oscillator input. The chosen input clock is distributed to two sets of outputs, providing clock configurations for double data rate 3 synchronous dynamic RAM (DDR3) and PCI-Express. Finally, a 50 MHz clock signal from the crystal oscillator is used to act as an external configuration clock to the FPGA.

2.3. System Technical Specifications

The radio signals processed by this system have a frequency range of 1–250 MHz, with a bandwidth ($f_{\max}$) of 250 MHz. According to the Nyquist theorem[10], the sampling rate should be at least twice the signal's bandwidth ($f_s \geqslant 2f_{\max}$) to fully recover the original signal. The AD9684BBPZ-500 acquisition card in this system employs a sampling rate of 500 Msps, precisely covering the 1–250 MHz frequency range of the HF-VHF dual-channel multifunctional radio astronomy terminal system.

Because different observational tasks require different frequency and time resolutions, the FFT points can be set to 32 768, 16 384, 8 192, or 4096. The frequency f can be calculated as

$$f = \frac{f_s}{N}, \tag{1}$$

where f_s is the sampling frequency and N is the number of samples.

The system's frequency resolution can be adjusted to approximately 16 kHz, 32 kHz, 64 kHz, or 128 kHz, and the time resolution can be set from 0.1 s and increased in steps of 0.1 s up to 5 s. Table 1 provides the main technical specifications of this dual-channel solar radio spectrum observation system.

Table 1. The main technical indicators of the HF-VHF band dual-channel multifunction radio astronomy terminal system

Sample/Msps	Frequency range/MHz	Spectral resolution/kHz	Temporal resolution/s	Number of FFT points
500	1–250	15.259	0.1–5	32 768
500	1–250	30.518	0.1–5	16 384
500	1–250	61.035	0.1–5	8 192
500	1–250	122.070	0.1–5	4 096

3. DESIGN OF THE RADIO ASTRONOMY TERMINAL SYSTEM

Existing spectrum analyzers are unable to simultaneously meet the requirements for remote data management, permission-based data sharing, solar radio spectrum analysis, time-domain recording for long-baseline interferometry, and asynchronous data playback. The HF-VHF dual-channel multifunctional radio astronomy terminal system discussed in this article is a data monitoring system designed for spectrum data analysis. This system's functionalities include data management, playback, analysis, visualization, storage, and acquisition. It uses a MySQL database as a unified system database and employs network transmission (TCP/IP) for data transfer. The system comprises two software components: a server and a client.

The client primarily handles data viewing, deletion, playback, analysis, and management. It generates waterfall plots, spectrograms, and time-domain graphs from the collected data and displays the status of server equipment. The server is responsible for data collection, processing, transmission, storage, and sending hardware status information to the client for display. During the data analysis process, the client receives data according to the configured parameters.

3.1. Server Design

The server primarily handles data collection, data transmission, data processing, data storage, and writes detailed information about the stored data files for management purposes. The server determines whether data has been collected by monitoring interrupts from the PCI-Express acquisition card. If data have been collected, it separates the data for channels one and two. During the separation process, spectral data undergo FFT calculations and energy integration according to the frequency and time resolutions set by the administrator. Meanwhile, time-domain data undergo data-shifting operations during the separation process. The entire workflow is illustrated in Fig. 5.

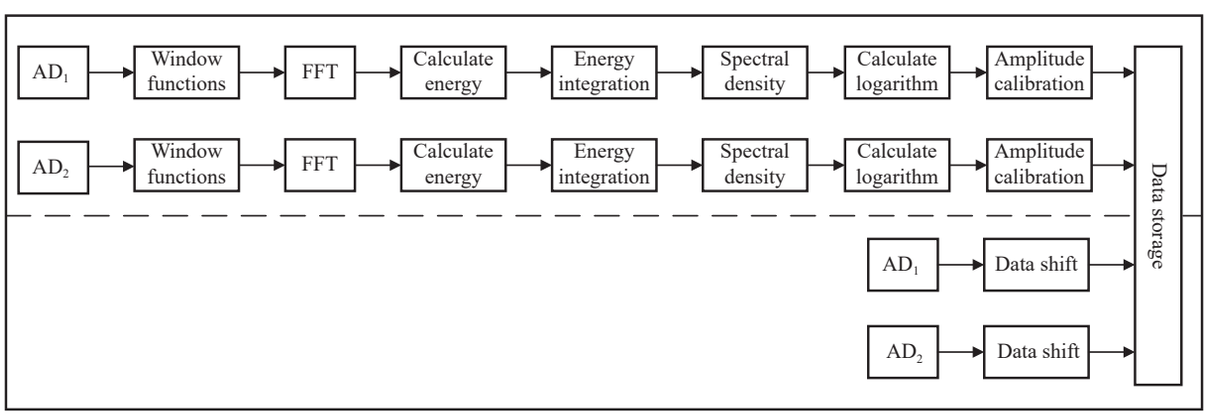

Fig. 5. Data processing flow chart.

In this system, each frame of time-domain data consists of 1 024 samples, while each frame of spectral data contains 16384 samples. After processing a frame of data, it is stored in the data repository, joining the data in the echo field.

3.1.1. *Signal windowing*

When the system conducts spectral analysis or time-frequency analysis on signals, various factors such as data volume, processing speed, and computational performance limit the system's ability to process the entire acquired digital signal. Consequently, the system truncates the signal, selecting a finite duration of data samples for analysis. This truncation process introduces additional spectral components, which can interfere with or mask the true spectral characteristics of the signal, resulting in inaccurate spectral analysis. This effect is known as spectral leakage[11].

To mitigate the impact of spectral leakage, considering that the number of sampling points is constrained by computational resources, the system uses windowing to reduce abrupt changes in the signal at its edges, thereby smoothing the signal and reducing the appearance of additional spectral components during analysis[12]. The window time-domain plots and frequency domain plots for rectangular, Hanning, Hamming, and Blankman windows are shown in Figs. 6, 7.

Given that the measurements in the HF-VHF dual-channel multifunctional radio astronomy terminal system involve random signals, the Hanning window is often used owing to its moderate main-lobe width, which provides reasonable frequency resolution[13]. Additionally, the Hanning window has relatively small side-lobe amplitudes, which helps suppress spectral leakage and side-lobe effects. The expression for the Hanning window is provided by

$$w(n)=\begin{cases}0.5\left(1-\cos\dfrac{2\pi n}{M-1}\right) & -M\leqslant n\leqslant M\\ \mathbf{0} & \text{other}\end{cases}, \quad (2)$$

where $w(n)$ represents the value of the Hanning window at discrete time point n and M denotes the window length

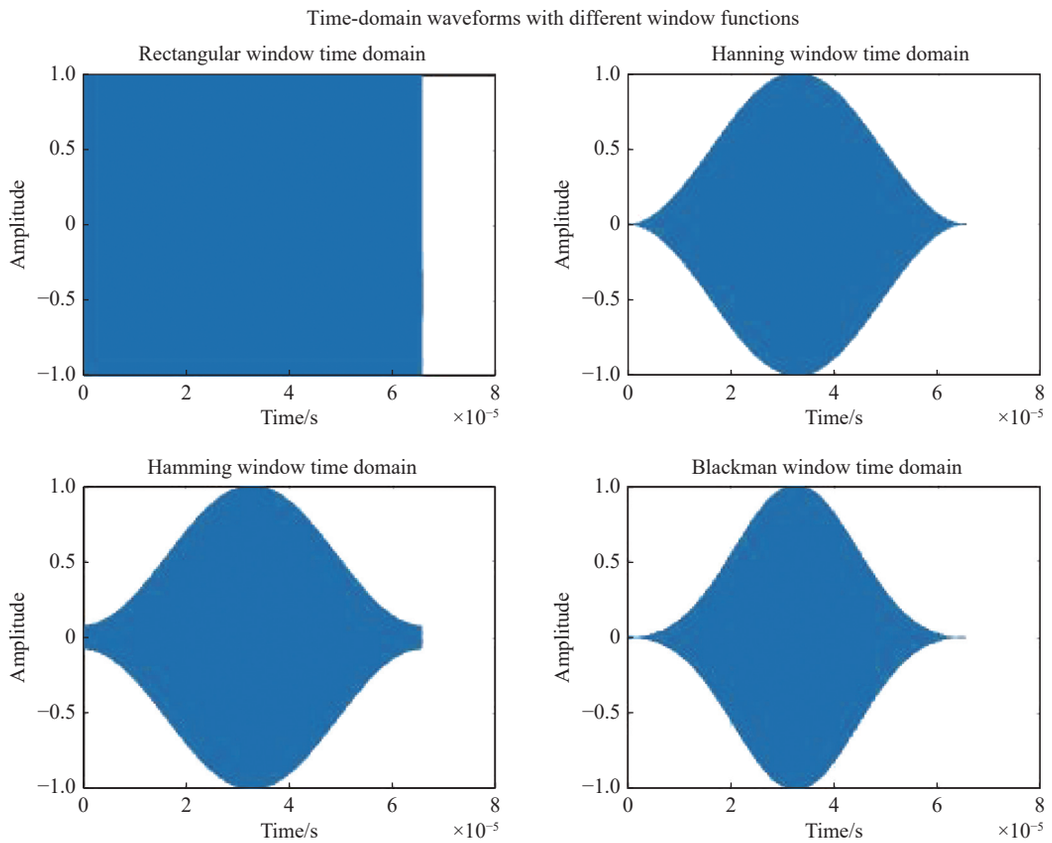

Fig. 6. Time-domain graph waveforms for rectangular, Hanning, Hamming, and Blankman windows.

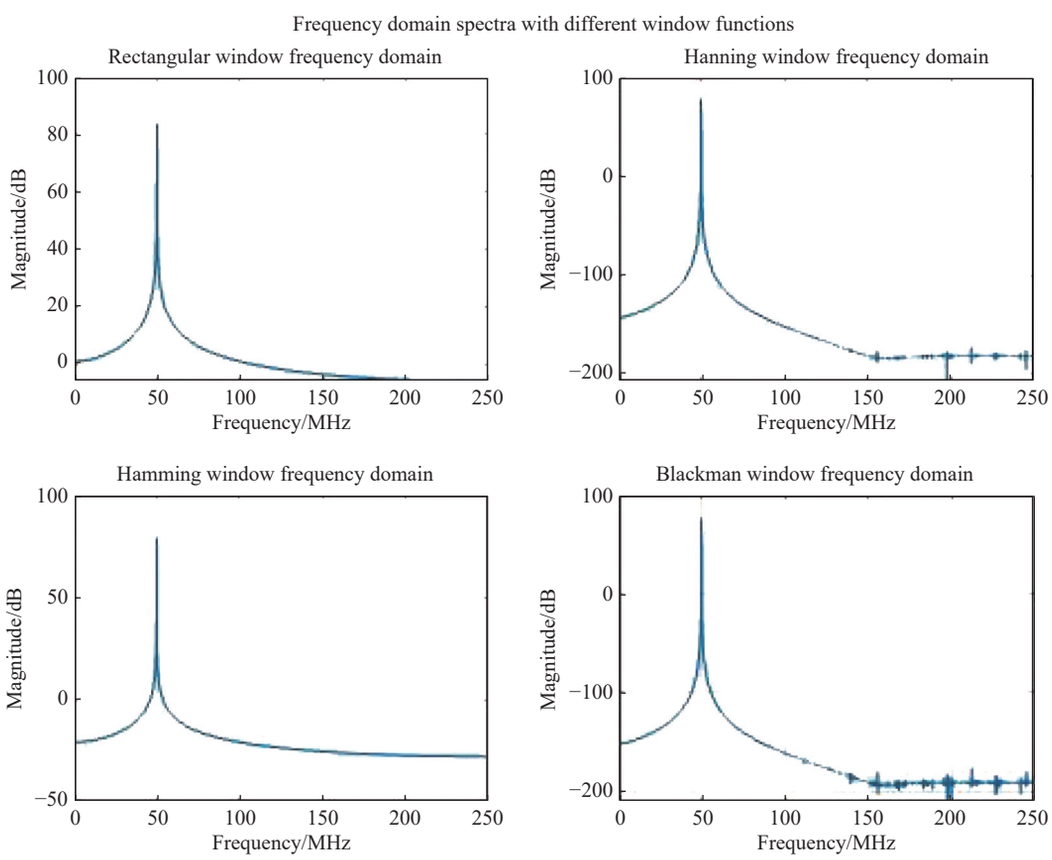

Fig. 7. Frequency domain waveform for rectangular, Hanning, Hamming, and Blankman windows.

(the window's size). The Hanning window can be considered as a cosine function centered around 0.5. Indeed, for the Hanning window, when $n = M-1$, the window takes on its minimum value of 0. When $n = (M-1)/2$, the Hanning window reaches its maximum value of 1.

The windowing process involves multiplying the input signal to obtain the windowed signal by a window function, as defined by

$$y(n) = x(n) \cdot w(n). \tag{3}$$

In this equation, $y(n)$ represents the value of the signal after being windowed with the Hanning window function, $x(n)$ is the original signal value, and $w(n)$ is the value of the Hanning window at the discrete time point n.

3.1.2. *FFT overlapping averaging algorithm*

According to the FFT algorithm[14], the signal $y(n)$ obtained after windowing is considered as a complex sequence of length $N\{x[0], x[1], x[2], \ldots, x[x-2], x[x-1]\}$. Its discrete Fourier transform (DFT) can be computed using the FFT algorithm, as defined by

$$X[k] = \sum_{n=0}^{n-1} x[n] W_N^{nk}. \tag{4}$$

In the equation, k is the index in the frequency domain, $X[k]$ represents the complex value in the frequency domain, n is the index in the time domain, $x[n]$ represents the complex value in the time domain, and N is the length of the sequence. The fundamental idea is to decompose the DFT into multiple smaller-scale DFTs and then recursively combine these smaller-scale DFTs to obtain the overall spectral result.

The length N of the FFT sequence can be selected from among powers of 2 within the range of 8 to 65 536. The system offers data sampling precision and phase factor precision ranging from 8 to 34 bits, and the computed results can be output with various levels of precision, including full-precision integers, scaled integers, or block floating-point formats. Considering all these factors, the system defaults to using a 32 768-point FFT with 14-bit full precision (adjustable to 16 384 points, 8 192 points, or 4 096 points, and 8-bit or 4-bit precision). As calculated by equation (1), this configuration yields a frequency resolution of 15.26 kHz, rounded to 16 kHz. For each point, FFT calculation results occupy 2 B of storage space according to 14 bits, the high-speed ADC sampling rate is 500 MHz, dual-channel simultaneous data acquisition, the data rate is calculated as 1 000 MB by

$$F_{\mathrm{n}} = f_{\mathrm{s}} \times ch \times B \times 50\%. \tag{5}$$

Here, F_{n} represents the data rate, f_{s} is the sampling rate, ch is the number of channels, and B is the number of bytes occupied by a single FFT calculation result. Owing to the symmetric nature of FFT, only 50% of the data are considered effective.

Given the high data rate and the associated storage and data transmission demands, an approach that averages the FFT results using the time resolution compression method has been chosen to address the challenge. This approach is represented by

$$\overline{X} = \frac{\sum_{i=0}^{N_t} X_i}{N_t} \tag{6}$$

and it aims to eliminate noise and reduce the data rate. Here, N_t represents the number of FFT result points within a unit of time resolution, X_i is the amplitude of a single FFT result, and $\overline{X}$ denotes the average amplitude of frequency points per unit time. The system's minimum time resolution is 0.1 s. This approach allows for data compression and noise reduction by averaging the FFT results within the specified time resolution.

3.2. Time-frequency Unit Design

The HF-VHF dual-channel multifunctional radio astronomy terminal system uses an integrated time-frequency unit consisting of a network time protocol (NTP) server, global positioning system (GPS) clock, 1 pulse per second (PPS) signal, and a 10 MHz signal. These components work in coordination to provide accurate time and frequency references.

The GPS clock ensures precise time reference, the 1 PPS signal is used for clock synchronization, and the 10 MHz signal serves as a frequency reference. The NTP server is responsible for transmitting time information to other devices within the terminal system, ensuring time synchronization and frequency consistency across the entire system.

The system periodically checks the status of the GPS clock, 1 PPS signal, and 10 MHz signal, performing these checks every second. If no external signals are detected, the display indicator lights turn red, and the data frame header position is set to 0. Additionally, the system initiates a time synchronization request to the NTP server every minute. If the request fails, the display indicator lights will also turn red. This comprehensive approach ensures that the system remains synchronized in terms of time and frequency.

4. MAIN PERFORMANCE METRICS TESTING

The HF-VHF band dual-channel multifunctional radio astronomy terminal system designed in this paper is tested to measure the main functional indices of the system as frequency resolution, time resolution, dynamic range, calibration test, and data storage function.

4.1. Frequency Resolution

Frequency resolution refers to the ability of a digital

signal processing system to distinguish between the closest two frequency components. To verify the frequency resolution, a signal source is used as an input for monitoring. A signal generator outputs a specific signal, and the system reads the frequency and amplitude of the signal's peak as well as the left and right side peaks to test the frequency resolution of the system and the accuracy of the acquired frequencies.

Table 2 shows the actual power of signals acquired by the vertical polarization channel of the HF-VHF dual-channel multifunctional radio astronomy terminal system. It evaluates the system's actual frequency resolution. The observed frequency range is 1−250 MHz, with a calculated frequency resolution of 16 kHz and a time resolution of 0.1 s. The recorded values of the left and right side peaks relative to the peak show a frequency difference of approximately 16 kHz and a power difference of more than 3 dB. This indicates that the system can differentiate between two frequency components separated by this frequency resolution.

Table 2. The actual power of the signal acquired by the vertical polarization channel of the HF-VHF band dual-channel multifunction radio astronomy terminal system

Signal frequency /MHz	Signal power /dBm	Measured frequency /MHz	Measured power /dBm	Resolution /K	Left sub-maximum frequency/MHz	Left sub-maximum power /dBm	Right sub-maximum frequency /MHz	Right sub-maximum power /dBm
150.000	0	150.000	−14.41	16	149.978	−27.25	150.024	−34.90
149.984	0	149.981	−13.42	16	149.966	−24.60	150.008	−35.88
150.016	0	150.016	−14.42	16	149.995	−29.12	150.039	−32.00
240.000	0	240.000	−10.72	16	239.976	−32.21	240.022	−26.17
239.984	0	239.980	−10.69	16	239.962	−28.16	240.006	−26.41
240.016	0	240.016	−10.58	16	239.996	−26.68	240.037	−24.27

4.2. Dynamic Range

Dynamic range, as a performance metric for measuring signal amplitudes, is defined as the ability of the spectrum analyzer's input to simultaneously measure the maximum and minimum signals, characterizing its capability to determine the amplitude difference between two concurrently present signals.

The minimum power is determined using a signal generator, starting from −30 dBm and decreasing by 1 dBm with each successive step. At each step, the system observes the detected power, ensuring that the power fluctuation remains below 1 dBm, and no significant deviation from the transmitted power is observed. The minimum power is recorded, and a similar procedure is followed to determine the maximum power.

Table 3 records the dynamic range of the signal measurements by the vertical polarization channel of the HF-VHF dual-channel multifunctional radio astronomy terminal system. As shown in Fig. 8, it represents the change in measured power with varying input power for different input frequencies.

Table 3. The dynamic range of the vertical polarization channel measurement signal of the HF-VHF band dual-channel multifunction radio astronomy terminal system

Signal frequency /MHz	Signal power /dBm	Measured frequency /MHz	Measured power/dBm
62.500	10.00	62.500	−2.00
62.500	0.00	62.500	−12.00
62.500	−10.00	62.500	−22.00
62.500	−30.00	62.500	−42.00

4.3. Calibration Testing

Absolute calibration is a special form of calibration for spectrum analysis systems designed to determine the absolute measurement values of the system, rather than relative measurement values. Absolute calibration typically employs known reference sources or standard signals to establish the system's absolute measurement scale. In this case, a broadband RF noise source (9 kHz to 3 GHz) is used to perform absolute calibration on the HF-VHF dual-channel multifunctional radio astronomy terminal system. Following calibration, tests are conducted, the frequency domain plot of the absolute calibration signal is shown in Fig. 9.

Calibration testing is a crucial step to ensure that the system can accurately measure and analyze spectrum signals. In this process, a known frequency and amplitude signal generator is used to produce a known, traceable reference signal. The system captures the calibration signal and records the obtained spectrum data, including the measured frequency and power, as well as the noise frequency and power. The results are documented in Table 4. Calibration testing validates the system's accuracy, precision, and reliability.

5. OBSERVATION RESULTS, ANALYSIS, AND PRESENTATION

The HF-VHF band dual-channel multifunctional radio astronomy terminal system is connected to the array antennas. The real-time spectra of horizontally polarized and vertically polarized radio signals are shown in Fig. 10. The time-domain diagram takes time as the horizontal axis

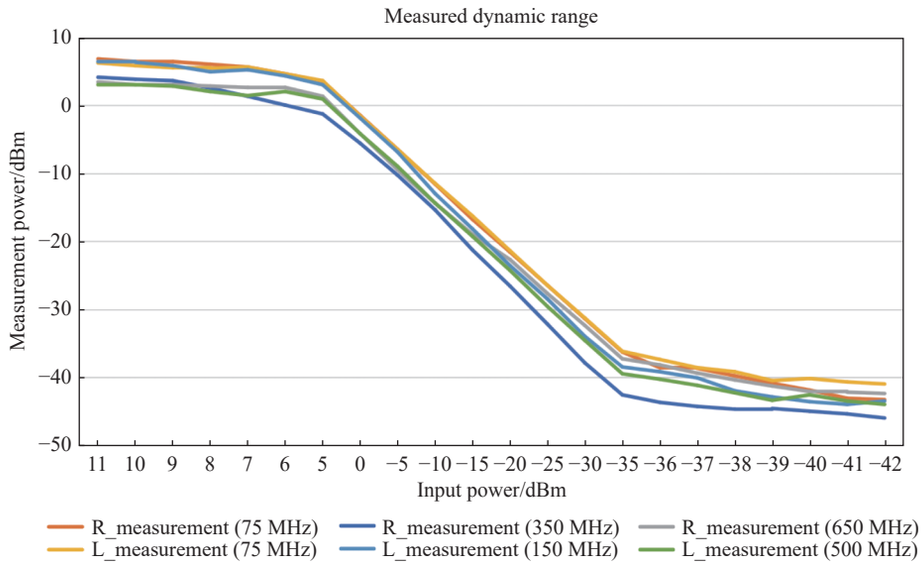

Fig. 8. Measured dynamic range of signal power.

Table 4. Vertical polarization channel calibration test of the HF-VHF band dual-channel multifunctional radio astronomy terminal system

Signal frequency /MHz	Signal power /dBm	Measured frequency /MHz	Measured power /dBm	Noise frequency /MHz	Noise power /dBm
10.000	−10.00	10.000	−21.72	19.9932	−81.18
10.000	−50.00	10.000	−60.72	30.0018	−92.20
100.000	−10.00	100.001	−27.73	79.9937	−93.13
100.000	−50.00	100.000	−65.37	110.001	−89.12
200.000	−10.00	200.000	−17.86	210.004	−86.38
200.000	−50.00	200.000	−55.72	210.004	−85.18

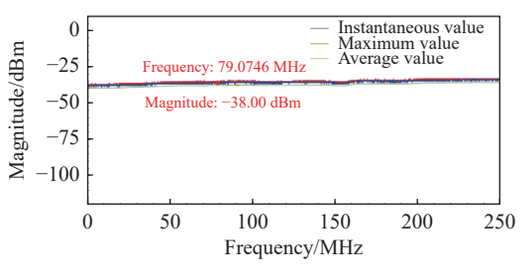

Fig. 9. Absolute calibration frequency domain diagram.

and the amplitude of the signal as the vertical axis, providing a visual display of the signal waveform and allowing observers to see changes in the signal in real time.

The radio signals are monitored as shown in the waterfall diagram in Fig. 11, generated by the software backtracking function. Here, the horizontal axis represents time, the vertical axis shows frequency, and colors represent signal strength at specific times and frequencies, which can capture and analyze transient events occurring.

6. CONCLUSION

After conducting comprehensive tests on the frequency resolution, time resolution, dynamic range, calibration test, display interface, long-term stability of the HF-VHF band dual-channel multifunction radio astronomical terminal system, we preliminarily determine that the system can handle the monitoring and research of solar radio signals in the China-Malaysia Joint Astronomy Project. The system has a wide frequency coverage from 1 to 250 MHz, with a sampling rate up to 500 Msps, a maxi-

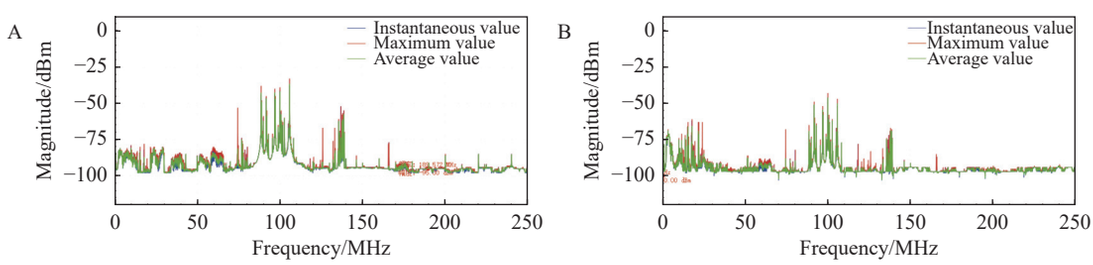

Fig. 10. Time-domain data observation diagram. (A) Time-domain data observation diagram of vertical polarization; (B) Time-domain data observation diagram of horizontal polarization.

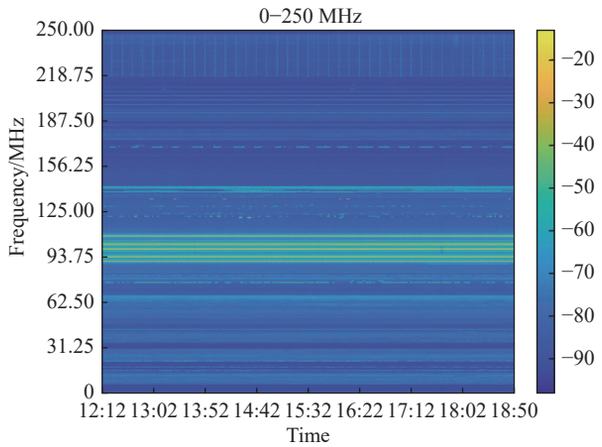

Fig. 11. Waterfall diagram generated by the backtracking function, showing variation in signal strength with time and frequency.

mum of 14 bits of quantization, a maximum time resolution of 0.1 s, and a maximum spectrum resolution of 16 kHz. In addition, the system runs in a server-client separation mode, allowing users to perform remote operations according to their respective permissions, including data viewing and observation plan making. The test results show that the system has excellent performance in signal processing and analysis. Its flexibility and practicality enable users to monitor and manage data anytime and anywhere, making it convenient for astronomical observations and data analysis.

At present, there are still some deficiencies the system. During remote data transmission, there are potential security risks that may threaten the integrity and confidentiality of data. In response to this issue, the system plans to protect data transmission by implementing encryption technology and security protocols to ensure the security of data. This measure aims to reduce the risk of unauthorized access or tampering with data.

The HF-VHF dual-channel multifunctional radio astronomical terminal system, with its advanced features, can perform precise signal detection and data acquisition within the HF-VHF frequency range. The efficient acquisition and processing capabilities of the system make it an indispensable tool for astronomers to study the dynamics and evolutionary properties of the universe.

ACKNOWLEDGEMENTS

This work was supported by National Natural Science Foundation of China (U2031133); National Key Research and Development Program of China (11941003); Applied Basic Research Program of Yunnan Province (2019FB009); Basic Research Program of Yunnan Province (202301AT070325); Square Kilometer Array (SKA) Project of the Ministry of Science and Technology of China (2020SKA0110202); International Partnership Program of the Chinese Academy of Sciences (114A11KYSB20200001); and Kunming Municipal Foreign (International) Cooperation Base Project (GHJD-2021022).

AUTHOR CONTRIBUTIONS

Kaijing Liu wrote the manuscript. Liang Dong supervised and organized the manuscript. Huanhuan Xie and Baoxin Li provided algorithmic technical support. Jingzhi Zhou proposed a writing strategy and revised the article. All authors read and approved the final manuscript.

DECLARATION OF INTERESTS

The authors declare no competing interests.

REFERENCES

[1] Zhang, X. M. 2021. The development in seismic application research of VLF/LF radio waves. *Acta Seismologica Sinica*, **43**(5): 656−673. (in Chinese)

[2] Oberoi, D., Kasper, J. C. 2004. LOFAR: the potential for solar and space weather studies. *Planetary and space science*, **52**(15): 1415−1421.

[3] Li, Y. 2015. Observations and modeling of solar flare atmospheric dynamics. *Acta Astronomica Sinica*, **56**(5): 528−530. (in Chinese)

[4] Yang, M. F., Wang, J. X.,Wang, C., et al. 2023. Envisioning the solar stereo exploration mission. *Chinese Science Bulletin*, **68**(8): 859−871. (in Chinese)

[5] Wu, K., Xu, J. Y., Yuan, W. 2023. Evolution of equatorial plasma bubbles group simultaneously observed by multi-instruments over China. *Chinese Journal of Space Science*, **43**(3): 446−455. (in Chinese)

[6] Zhang, J. P., He, L. S., Dong, L., et al. 2016. The design and implementation of a low frequence radio antenna array digital terminal. *Astronomical Research & Technology*, **13**(2): 170−177. (in Chinese)

[7] Zhang, Y. B., Wu, J., Xu, Z. W., et al. 2018. Influence of ionospheric E on radio propagation in HF and VHF band. *Chinese Journal of Space Science*, **38**(6): 879−885. (in Chinese)

[8] Berngardt, O. I., Lebedev, V. P., Kutelev, K. A., et al. 2018. First joint observations of radio aurora by the VHF and HF radars of the ISTP SB RAS. *Radiophysics and Quantum Electronics* , **60**(8): 618−639.

[9] Ping, J. S., Wang, M. Y., Zhang, M., et al. 2021. Introduction of space exploration progress for planetary radio burst emission. *Journal of Deep Space Exploration*, **8**(1): 80−91. (in Chinese)

[10] Shan, G. J. 2020. The study of signal reconstruction: an investigation independent of Shannon-Nyquist theorems. *Science China(Information Sciences)*, **63**(10): 279−281.

[11] Chen, Y. P., Xie, Y. H., Zhou, Q. W., et al. 2022. Designing mean parameter measurement window based on signal harmonic characteristics. *Journal of Xi'an Jiaotong University*, **56**(5): 191−198. (in Chinese)

[12] Liu, X. J., Zhou, G., Lu, W. L., et al. 2023. Application of windowed weighted interpolation discrete Fourier transform in wavelength scanning interferometer. *Journal of Huazhong University of Science and Technology (Natural Science Edition)*, **51**(6): 41−47. (in Chinese)

[13] Wang, Y. L., Shi, Y. B., Kang, Q., et al. 2019. Frequency extraction and correction based on double-window all-phase FFT of laser Doppler. *Laser & Infrared*, **49**(12): 1395−1401. (in Chinese)

[14] Zhao, X., Jia, H. P., Zhang, Y. Q., et al. 2023. Real FFT implementation and performance optimization based on ARMv8 CPUs. *Chinese Journal of Computers*, **46**(5): 1003−1018. (in Chinese)